Published online 19 December 2011 *Nucleic Acids Research, 2012, Vol. 40, No. 8* **3563–3573**
doi:10.1093/nar/gkr1237

Topo IV is the topoisomerase that knots and unknots sister duplexes during DNA replication

Virginia López, María-Luisa Martínez-Robles, Pablo Hernández, Dora B. Krimer and Jorge B. Schvartzman*

Departamento de Proliferación Celular y Desarrollo, Centro de Investigaciones Biológicas (CSIC), Ramiro de Maeztu 9, 28040 Madrid, Spain

Received October 10, 2011; Revised and Accepted November 29, 2011

ABSTRACT

DNA topology plays a crucial role in all living cells. In prokaryotes, negative supercoiling is required to initiate replication and either negative or positive supercoiling assists decatenation. The role of DNA knots, however, remains a mystery. Knots are very harmful for cells if not removed efficiently, but DNA molecules become knotted *in vivo*. If knots are deleterious, why then does DNA become knotted? Here, we used classical genetics, high-resolution 2D agarose gel electrophoresis and atomic force microscopy to show that topoisomerase IV (Topo IV), one of the two type-II DNA topoisomerases in bacteria, is responsible for the knotting and unknotting of sister duplexes during DNA replication. We propose that when progression of the replication forks is impaired, sister duplexes become loosely intertwined. Under these conditions, Topo IV inadvertently makes the strand passages that lead to the formation of knots and removes them later on to allow their correct segregation.

INTRODUCTION

Among the three classical DNA topological forms: supercoils, catenanes and knots, the former two are a direct consequence of fundamental DNA metabolic processes: transcription and replication (1). They were early recognized as soon as the model for the DNA double helix was originally proposed (2). DNA knots, on the other hand, although recognized even before (3), arise mainly as a by-product of topoisomerase II-mediated double-stranded passages (4). Knots in DNA have potentially devastating effects for cells (5,6) and therefore need to be quickly removed.

DNA knots, however, form *in vivo* in non-replicating-cells (7–9) and also during replication (10–14). It is important to distinguish, though, between unreplicated circular molecules with intramolecular knots and partially replicated molecules with intra- or interchromatid knots (Figure 1A and B). Although type-I DNA topoisomerases and DNA gyrase can knot and unknot DNA duplexes *in vitro* (15), it is firmly established that *in vivo*, Topo IV is the only topoisomerase significantly involved in decatenation and unknotting of DNA molecules (16–20). But how and why DNA becomes knotted in the first place is not entirely understood. Here, we show that Topo IV is also the topoisomerase that makes knots during DNA replication. This observation implies an unforeseen paradox, as the same enzyme that knots DNA is responsible for their removal later on, consuming ATP in both processes.

MATERIAL AND METHODS

Bacterial strains, plasmids and culture medium

The *E. coli* strains used in this study and their relevant genotype are detailed in Supplementary Table S1. Competent cells were transformed with monomeric forms of pBR-TerE@StyI, pBR-TerE@AatII, or pBR-TerE@DraI, all derivatives of pBR322 with the polar replication terminator TerE (21,22) cloned at variable distances from the unidirectional ColE1 origin. All the strains were grown in LB medium at 37°C with the exception of parE10 cells, which were grown at the permissive (30°C) or restrictive (43°C) temperature. Isolation of plasmid DNA was performed as described elsewhere (12,23).

DNA treatments

To induce single-stranded breaks, DNA was digested with Nb.BsmI, Nb.BtsI, Nt.BbvCI (New England Biolabs) or Nt.Bpu10I (Fermentas) for 30 min at 37°C. Reactions were blocked with 100 $\mu g\,ml^{-1}$ proteinase K (Roche) for 30 min at 37°C. Digestions with AlwNI (New England

*To whom correspondence should be addressed. Tel: +34 91 837 3112 (ext. 4232); Fax: +34 91 536 0432; Email: schvartzman@cib.csic.es

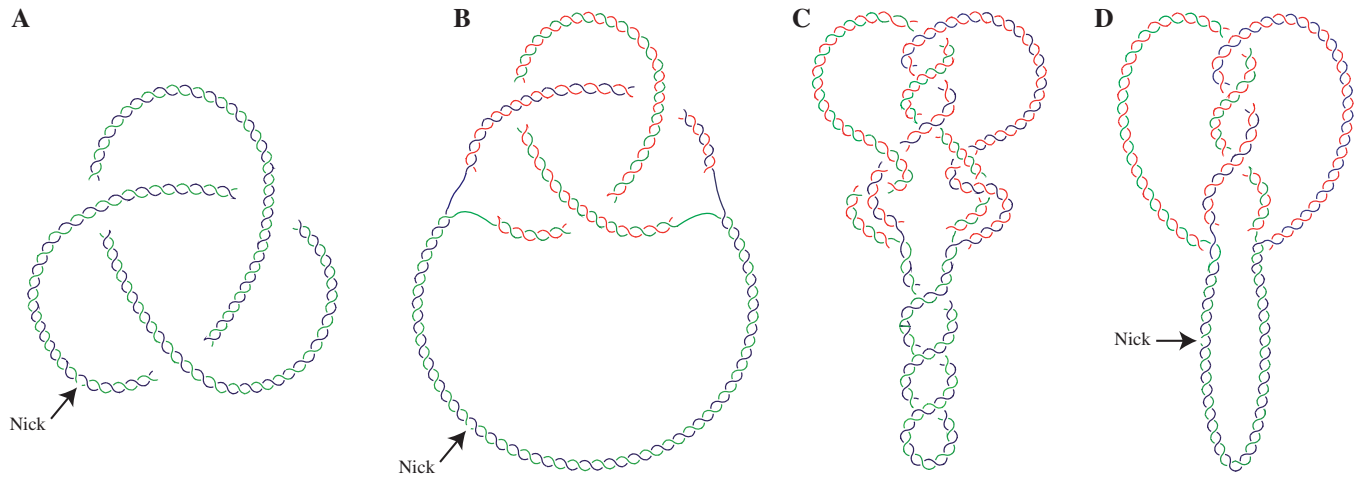

Figure 1. Cartoons illustrating the topology of different DNA molecules. (**A**) Unreplicated circular nicked molecule displaying an intramolecular trefoil knot. (**B**) Partially replicated RI with a nick in the unreplicated portion containing an interchromatid trefoil knot. (**C**) Partially replicated CCRI displaying supercoiling in the unreplicated portion, catenanes and an interchromatid trefoil knot in the replicated portion. (**D**) Nicking in the unreplicated portion eliminates supercoiling and catenation revealing the interchromatid knot alone. Parental duplexes are indicated in blue and green and nascent strands are depicted in red.

Biolabs) and Topo IV (Inspiralis) were performed following manufacturer's instructions.

Two-dimensional agarose gel electrophoresis and Southern transfer

The first dimension was in a 0.4% agarose gel in TBE buffer at $0.9\,V\,cm^{-1}$ at room temperature for 25 h. The second dimension was in a 1% agarose gel in TBE buffer without ethidium bromide (EthBr) if the samples were analysed intact or containing $0.3\,\mu g\,ml^{-1}$ EthBr if the samples were digested with AlwNI. This second dimension was run perpendicular to the first dimension. The dissolved agarose was poured around the excised agarose lane from the first dimension and electrophoresis was at $5\,V\,cm^{-1}$ in a 4°C cold chamber for 10–13 h (8 h for those samples digested with AlwNI). Southern transfer was performed as described elsewhere (12,23).

Non-radioactive hybridization

Probes were labelled with digoxigenin using the DIG-High Prime kit (Roche). Membranes were prehybridized in a 20 ml prehybridization solution (2× SSPE, 0.5% Blotto, 1% SDS, 10% dextran sulphate and $0.5\,mgml^{-1}$ sonicated and denatured salmon sperm DNA) at 65°C for 4–6 h. Labelled DNA was added and hybridization lasted for 12–16 h. Then hybridized membranes were sequentially washed with 2× SSC and 0.1% SDS, 0.5× SSC and 0.1% SDS, 0.1× SSC and 0.1% SDS for 15 min each at room temperature except for the last wash, which took place at 65°C. Detection was performed with an antidigoxigenin-AP conjugate antibody (Roche) and CDP-Star (Perkin Elmer) according to the instructions provided by the manufacturer.

Densitometry

Autoradiograms were scanned and the region where unknotted and knotted RIs migrated was analysed by densitometry using NIH Image J64 to determine the ratio of knotted to unknotted molecules.

Preparation of DNA samples enriched for specific RIs

Plasmid DNA isolated from exponentially growing cells was nicked and analysed in a 1D low melt agarose gel (BioRad) run for 36 h under the conditions used for the first dimension of a regular 2D gel. An aliquot of the same sample was run in a separate lane and used as a control. After the first dimension, this control lane was cut out, stained with EthBr and examined under UV light. In this way, we estimated the distance migrated by the molecules of interest. According to this estimation, the portion of the gel containing these molecules was excised; the agarose melted at 65°C and digested with β-Agarase I (New England Biolabs). The remaining insoluble products were eliminated by centrifugation and the DNA sample was phenol extracted, ethanol precipitated and resuspended in distilled water.

Sample preparation and atomic force microscopy imaging

Sample DNAs were coated with RecA by mixing a ratio of 1 µl DNA, 6 µl ATPγS at a final concentration of $1\,mgml^{-1}$ (Sigma), and 8 µl of RecA (New England Biolabs) at a final concentration of $0.2\,mgml^{-1}$ (24). After incubation at 37°C for 1 h, 1–2 µl of the reaction mixture was deposited onto AP-mica—mica previously modified with 3-aminopropyltriethoxy silane (APTES)—as follows: freshly cleaved mica (Ted Pella, CA, USA) was treated with a 0.025% water solution of APTES (Sigma) for 1 min, rinsed thoroughly with ultrapure water (Millipore, MA, USA) and dried with a stream of compressed nitrogen. Then, an aliquot of the DNA sample coated with RecA was deposited onto AP-mica, incubated for about 1 min at room temperature, rinsed with ultrapure water and dried with a stream of compressed nitrogen. Images were collected using a Nanoscope IIIa

(Veeco, Woodbury, NY, USA) operated in tapping mode in air. The cantilevers (MPP-12120-10 Bruker Corporation, CA, USA) had a nominal tip radius smaller than 10 nm and exhibited resonant frequencies in the range of 100–200 kHz. During imaging, the surface was scanned at a rate of one line per second. The images were flattened to remove the eventual slope of the substrate using the Nanoscope software, and analysed with no further treatment. DNA molecules were analysed using Ellipse program version 2.08 (Institute of Experimental Physics, Kosice, Slovakia) to trace each molecule and to accurately measure the contour length.

RESULTS

As pointed out in the Introduction, our main tasks were to characterize the knots that form during DNA replication, to identify the topoisomerase responsible for knotting sister duplexes during DNA replication and to determine why they form in the first place. To study interchromatid knots in bacteria, we constructed three plasmids, all derivatives of pBR322, containing the *E. coli* replication terminator DNA sequence TerE (21,22) in its active orientation at three different sites: StyI, AatII and DraI. The resulting plasmids were named pBR-TerE@StyI, pBR-TerE@AatII and pBR-TerE@DraI, respectively. Blockage of the unidirectional replication fork at TerE, led to the accumulation of replication intermediates (RIs) with a mass 1.26×, 1.60× and 1.80× the mass of unreplicated molecules, respectively (see left side of Figure 2). As Topo IV is the topoisomerase that unknots DNA molecules *in vivo* (16–20), parE10 *E. coli* cells carrying a mutation in the *parE* gene that makes Topo IV temperature sensitive, were transformed with the three plasmids at the permissive temperature (30°C). When the cultures achieved logarithmic growth an aliquot

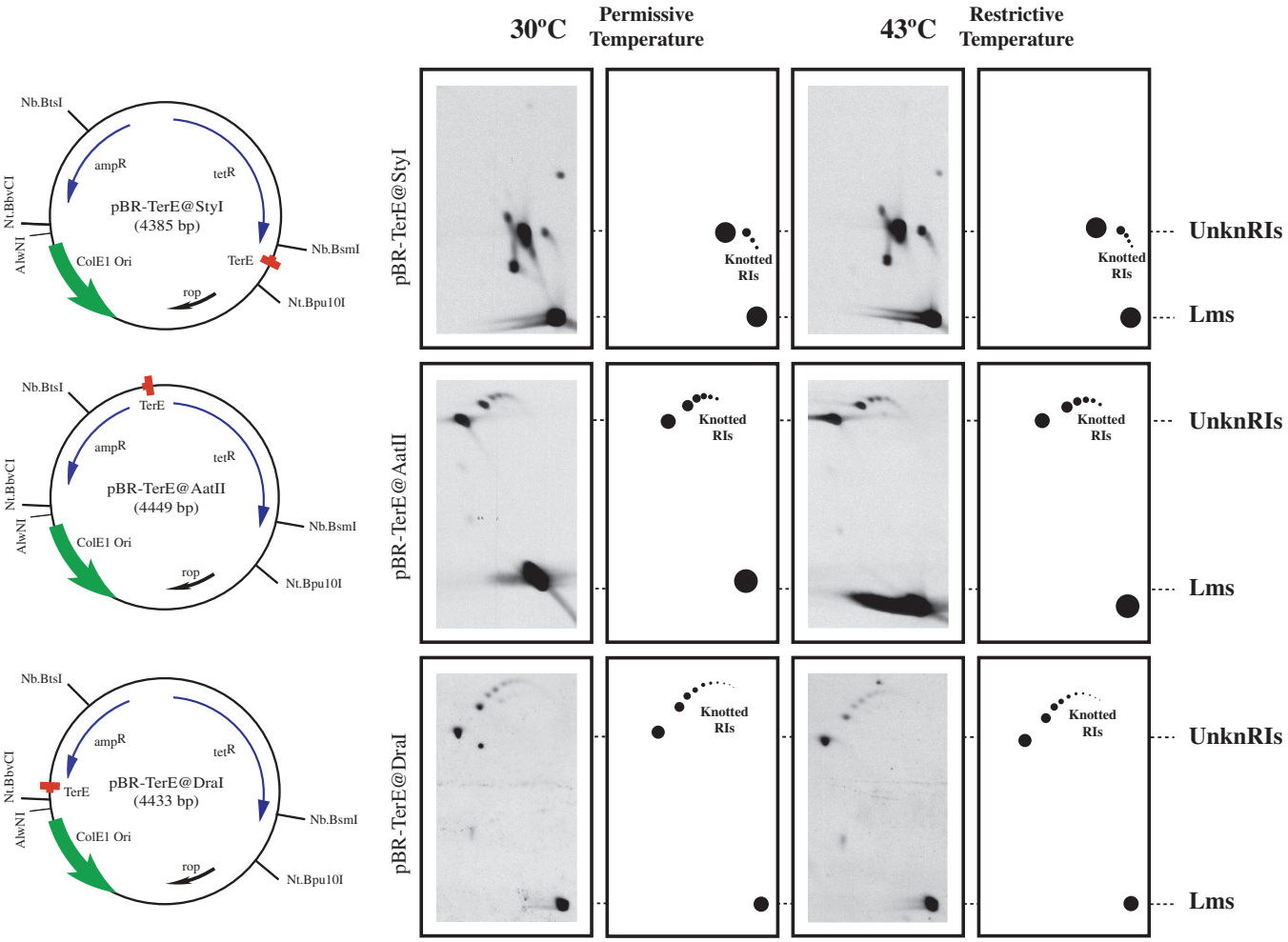

Figure 2. Identification of partially replicated molecules at different stages of replication containing interchromatid knots. The name, mass and genetic maps of the plasmids used are indicated on the left side. Inside, each map shows the relative position of its most relevant features: the ColE1 unidirectional origin (ColE1 Ori), the *E. coli* terminator sequence (TerE) and the ampicillin- and tetracycline-resistance genes (ampR and tetR). Outside, the relative positions of sites recognized by specific restriction endonucleases are indicated. Autoradiograms of plasmid DNAs isolated from parE10 cells grown at the permissive and restrictive temperatures after digestion with AlwNI and analysed in 2D gels with their corresponding interpretation diagrams are shown on the right side. For comparison autoradiograms were aligned according to the electrophoretic mobility of unknotted replication intermediates (UnknRIs) and linearized molecules (Lms). Note that no significant difference was observed between the samples taken from cells grown at the permissive or restrictive temperatures.

was taken and the cultures were shifted to the restrictive temperature (43°C) for another 60 min. To identify knotted RIs, the three plasmids were digested with AlwNI, a restriction endonuclease that cuts each plasmid only once in the unreplicated portion and analysed by 2D agarose gel electrophoresis as indicated elsewhere (25). The results obtained are shown on the right side of Figure 2. The resulting linearized plasmids contained an internal bubble, the size of which varied in each case (11,12,23). Note that in all cases no significant difference was observed between the samples taken from cells grown at the permissive temperature and those extracted from cells that were exposed to the restrictive temperature for 60 min. Comparison of the autoradiograms corresponding to the three plasmids indicated that the electrophoretic mobility of unreplicated forms was the same in all cases, which was expected for molecules of fairly similar sizes (4385 bp for pBR-TerE@StyI; 4449 bp for pBR-TerE@AatII; and 4433 bp for pBR-TerE@DraI). The electrophoretic mobility of unknotted and knotted RIs, on the other hand, varied significantly according to the size of the bubble (11). To confirm that Topo IV was inhibited at the restrictive temperature, cells transformed with pBR-TerE@DraI were visualized at a phase contrast microscope and undigested plasmid DNA was analysed by 2D agarose gel electrophoresis (Figure 3). The change in the shape of the cells (26,27) and the accumulation of catenated forms (28) confirmed that exposure of mutant cells to the restrictive temperature inhibited Topo IV in a significant manner.

To confirm the nature of the molecules identified as knotted RIs, two series of experiments were performed. In the first case, plasmids isolated from wild-type cells were analysed in 2D gels untreated and after digestion with a restriction enzyme that introduces a single-stranded break either at the replicated or at the unreplicated

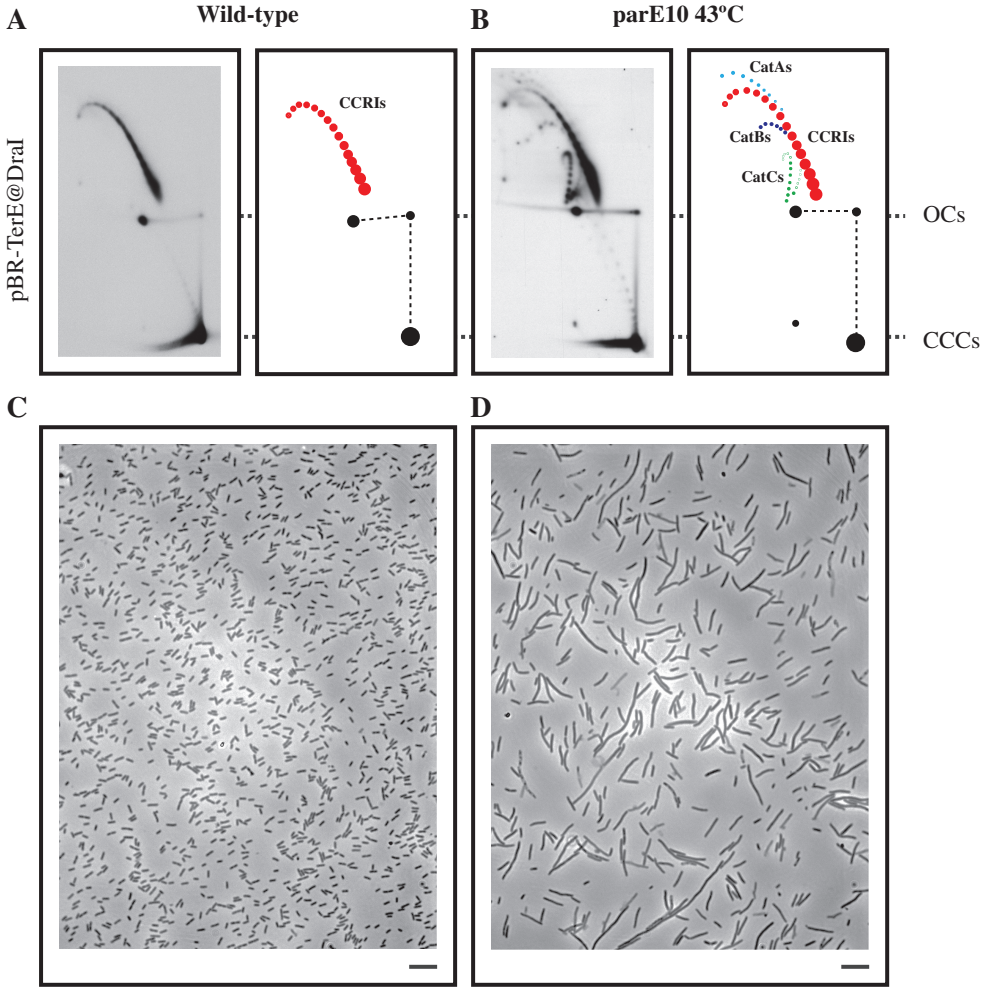

Figure 3. Exposure of parE10 *E. coli* cells to the restrictive temperature (43°C) leads to the specific inhibition of Topo IV, which in turns causes an accumulation of catenated molecules and progressive elongation of the cells. Autoradiograms of 2D gels corresponding to intact forms of pBR-TerE@DraI isolated from wild-type cells (**A**) and parE10 cells after a 60 minutes exposure to the restrictive temperature (**B**). Interpretative diagrams are shown to the right. Note the accumulation of CatAs (depicted in light blue), CatBs (depicted in dark blue) and CatCs (depicted in green) in the corresponding diagram. For comparison the autoradiograms were aligned so that the electrophoretic mobility of unreplicated open circles (OCs) and covalently closed circles (CCCs) coincided. Covalently closed replication intermediates (CCRIs) are depicted in red. The phase-contrast micrographs correspond to wild-type cells (**C**) and parE10 cells after a 60 min exposure to the restrictive temperature (**D**). Note the elongated shape of the cells in D. The bar is 10-μm long.

portion of the accumulated RIs. Each plasmid contained a single site for the nicking restriction endonuclease employed and their locations are indicated in the maps shown on the left side of Figure 2. In the second series of experiments, DNA samples enriched for specific DNA molecules (29–31) were prepared and analysed by atomic force microscopy (AFM).

The results obtained with intact plasmids and after nicking are shown in Figure 4. As in the autoradiograms shown in Figure 2, the signals corresponding to non-replicating forms showed the same electrophoretic mobility for the three plasmids. Here these signals corresponded to covalently closed circles (CCCs) and open circles (OCs), respectively. Similarly, the electrophoretic mobility of molecules with the fork blocked at TerE also varied according to the size of the bubble. Contrary to the autoradiograms shown in Figure 2, however, in this case the accumulated RIs consisted in a family of molecules with increasing mobility that formed a characteristic arc (coloured red in the corresponding diagrams in Figure 4). The different elements of these families have the same mass but differ in their linking number (Lk). As in all partially replicated molecules the forks rotate freely *in vitro*, the corresponding linkage is distributed between the unreplicated and replicated portions according to their relative sizes (Figure 2). Supercoils in the unreplicated portion and precatenanes in the replicated one determine Lk (32). Digestion of the samples with a nicking enzyme at either the replicated or unreplicated portions has one common consequence: for all the plasmids the signal corresponding to unreplicated CCCs disappeared (broken circles mark their position at the bottom right corner of the autoradiograms in Figure 4). This observation: (i) confirmed that the signals identified as CCCs corresponded

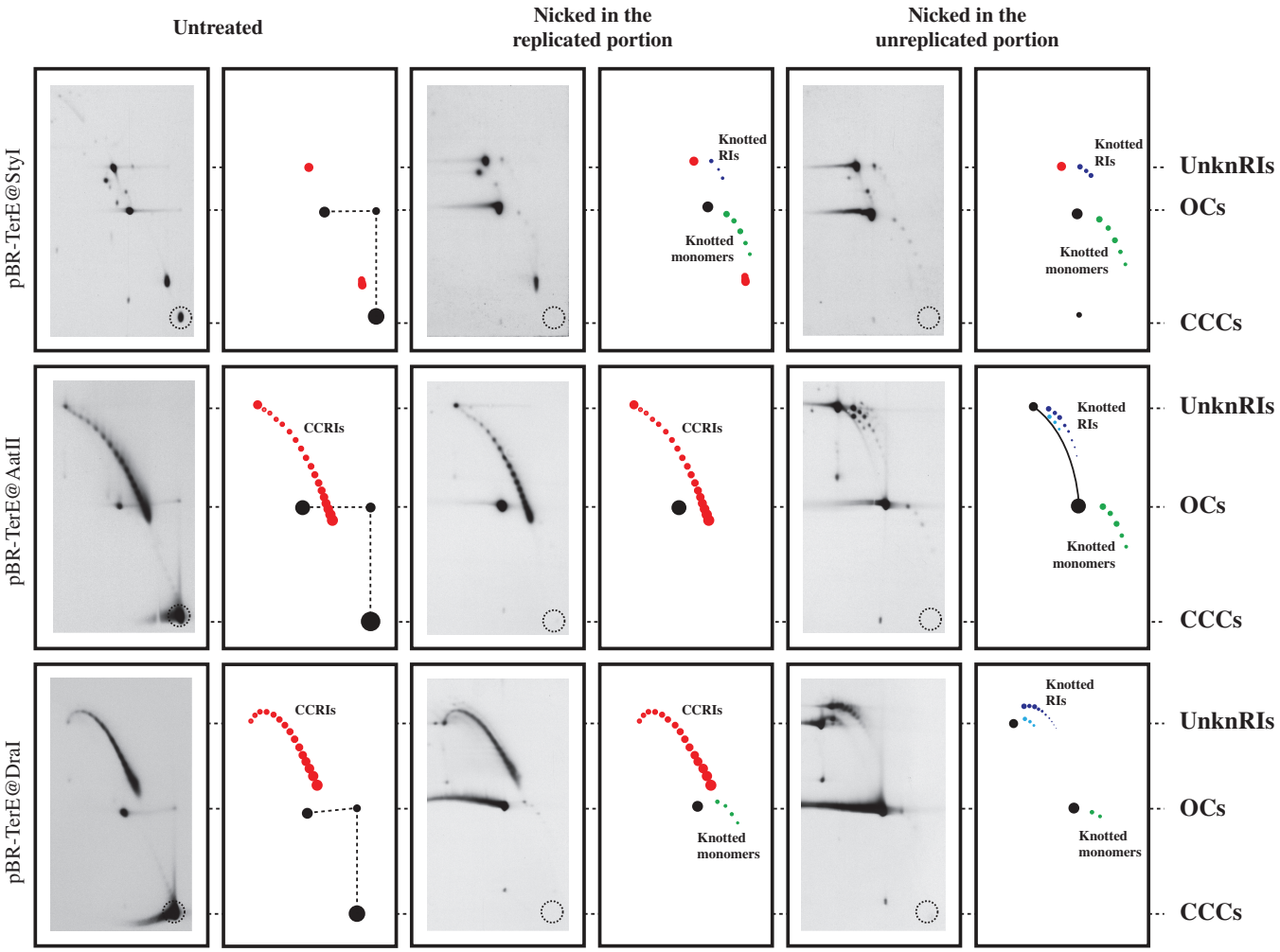

Figure 4. Nicking of intact circular RIs with single-stranded restriction endonucleases revealed knotted RIs only when the nicking occurred in the unreplicated portion. Plasmid DNAs isolated from parE10 cells grown at the restrictive temperature untreated and after digestion with restriction endonucleases that introduced a single-stranded break either in the replicated or unreplicated portions were analysed in 2D gels. The autoradiograms with their corresponding interpretation diagrams are shown. For comparison all autoradiograms were aligned according to the electrophoretic mobility of unknotted replication intermediates (UnknRIs), open circles (OCs) and covalently closed circles (CCCs). The signal corresponding to covalently closed replication intermediates (CCRIs) are indicated in red; knotted monomers corresponding to unreplicated forms are indicated in green and knotted replication intermediates (Knotted RIs) are indicated in dark and light blue. The dotted circle at the bottom right corner of each autoradiogram marks the electrophoretic mobility expected for unreplicated CCCs.

indeed to unreplicated monomeric CCCs; and (ii) served as an internal control indicating that digestions with the nicking enzymes were complete. The signals identified as OCs, on the other hand, persisted. Nicking revealed a new family of stereoisomers that corresponded to monomeric forms. Based on their electrophoretic mobility during the first and second dimensions they were identified as nicked knotted monomers (33) and are coloured green in the diagrams in Figure 4. Note that the signals called CCRIs remained unchanged after nicking at the replicated portion but disappeared when this nicking occurred at the unreplicated portion. This is precisely what is expected as in the replicated portion the nascent strands of the sister duplexes already contain interruptions due to the discontinuous nature of DNA synthesis of the lagging strands. For this reason, the introduction of a new nick at the replicated portion had no topological consequence. Nicking at the unreplicated portion, however, completely eliminated the signal corresponding to CCRIs. The introduction of a nick eliminates supercoiling because the torsional tension self-contained in CCRIs dissipates when the ends of the broken strands are allowed to swivel around the unbroken one. This automatically causes the forks to rotate to redistribute the Lk between the unreplicated and replicated portions. In this way precatenanes diffuse back to the unreplicated portion and the corresponding Lk is eliminated (Figure 1C and D). But inter- and intrachromatid knots cannot diffuse to the unreplicated portion and are distinctly revealed (Figure 4). In the corresponding diagrams dark and light blue arcs point to RIs containing simple and double knots, respectively (11).

To further confirm the nature of the so-called knotted RIs, DNA samples enriched for these molecular species were prepared (12,13,29–31), nicked at the unreplicated portion, coated with RecA (24) and examined by AFM. This technique allows a precise examination of individual molecules extended onto a flat surface. Moreover, as the molecules were nicked they contained no precatenanes and using enhanced contrast, the branches that pass above and below at each individual cross can be unambiguously identified (Figure 5). In this way, after measuring the length of the three arms, knotted and unknotted molecules were distinguished and classified. RIs corresponding to pBR-TerE@AatII are shown on the left of Figure 6. An unknotted RI is shown in Figure 6A. The molecule in Figure 6B although contains four nodes corresponds to an interchromatid trefoil knot where all the nodes have positive signs. The unmarked node corresponds to an accidental crossing that disappears after rotation of the fork. Finally, the molecule in Figure 6C corresponds to an RI with an intrachromatid knot. Examples of partially replicated molecules corresponding to pBR-TerE@DraI are shown on the right of Figure 6. An unknotted RI with no nodes is shown in Figure 6D. The molecules shown in Figure 6E and F display several nodes in 2D but their interpretative diagrams after 3D reconstruction indicated they corresponded indeed to unkotted RIs.

The observation for no apparent difference between the patterns generated by DNA extracted from cells grown at the permissive and restrictive temperatures shown in Figure 2, prompted us to investigate this problem in depth. To this aim, parE10 *E. coli* cells transformed with pBR-TerE@DraI were grown at the permissive temperature (30°C) until the cultures achieved logarithmic growth. A sample was taken and the cultures shifted to the restrictive temperature (43°C). More samples were taken 60 and 120 min after the temperature shift. Plasmid DNA was isolated, digested with AlwNI and analysed in 2D gels. Finally, the region of the autoradiogram where unknotted and knotted RIs migrated was scanned and analysed by densitometry to determine the ratio of knotted to

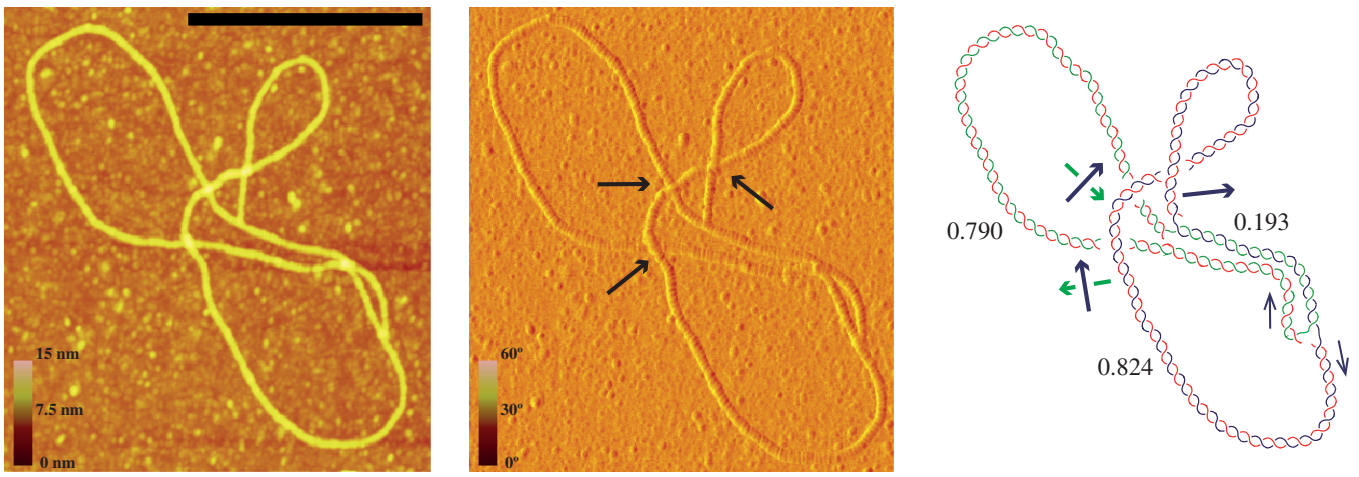

Figure 5. Atomic force microscopy (AFM) allows the unambiguous identification of the shape of individual molecules extended on a flat surface. Visualization of height-data and phase-data (left and middle photographs, respectively) distinguishes which branch is above and which below at each individual node (see blue arrows in the middle photograph). This is essential to determine whether the molecule is knotted or not. The interpretative diagram shown to the right confirmed that this molecule corresponding to pBR-TerE@DraI was unknotted. In the diagram the parental duplex is drawn in blue and green whereas the nascent strands are drawn in red. Numbers indicate the relative size of each arm. Black arrows mark directionality of the sister duplexes and green and blue arrows indicate handedness. The scale on the left of the photographs represents height and phase and the black bar is 250-nm long.

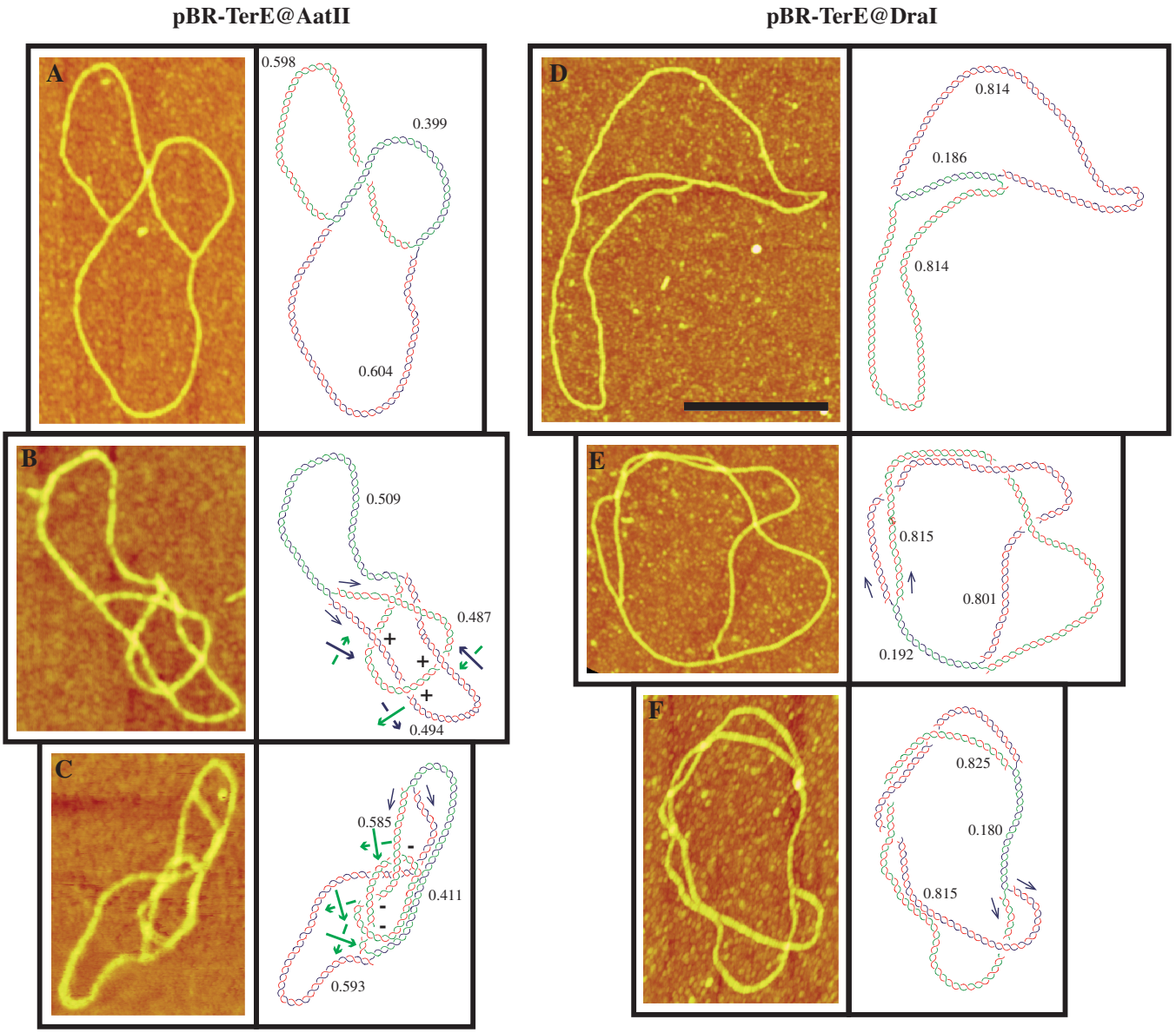

Figure 6. Partially replicated unknotted and knotted molecules corresponding to pBR-TerE@AatII (on the left) and pBR-TerE@DraI (on the right) as visualized by atomic force microscopy (AFM). DNA samples enriched for plasmid DNAs isolated from parE10 cells grown at the restrictive temperature were digested with restriction endonucleases that introduced a single-stranded break at the unreplicated portion, coated with RecA and analysed by AFM. In the interpretative diagrams (shown to the right of each photograph) the parental duplex is drawn in blue and green and the nascent strands are drawn in red. Numbers in the interpretation diagrams indicate the relative size of each arm. Black arrows mark directionality of the sister duplexes. Green and blue arrows indicate handedness and the signs specify whether the node is negative or positive. (**A**) and (**D**) Unknotted RIs; (**B**) Partially replicated molecule with an interchromatid trefoil knot where all the nodes have a positive sign; (**C**) Partially replicated molecule with an intrachromatid knot; (**E**) and (**F**) Partially replicated molecules displaying several nodes in 2D. The interpretation diagrams, though, indicated they indeed corresponded to unknotted RIs. The scale on the left of (A) represents height and the black bar in (D) is 250-nm long.

unknotted molecules. The results obtained are shown in Figure 7. The ratio remained almost unchanged (0.50, 0.50 and 0.49, respectively) with time. Although type I topoisomerases can knot nicked or gapped templates (15), it is generally accepted that knotting *in vivo* is mainly caused by a type II DNA topoisomerase (4) and in bacteria, there are only two potential candidates: DNA gyrase and Topo IV. If the topoisomerase responsible for making these replication knots would be DNA gyrase, as Topo IV, which is the topoisomerase responsible for unknotting (16–20), was inhibited in these cells (Figure 3), the ratio of knotted to unknotted RIs should had gone up with time. This was not the case. Knotted RIs could also form as a by-product of interchromatid recombination catalyzed by XerC and XerD (34). To test if the latter recombination system was involved in the formation of interchromatid knots, *xerC* and *xerD* mutant *E. coli* cells were transformed with the same plasmid and the experiment repeated. If XerC and/or Xer D were somehow involved in the formation of interchromatid knots, no knotting would take place in the mutant cells and the ratio of knotted to unknotted RIs should go down. On the contrary, the results shown

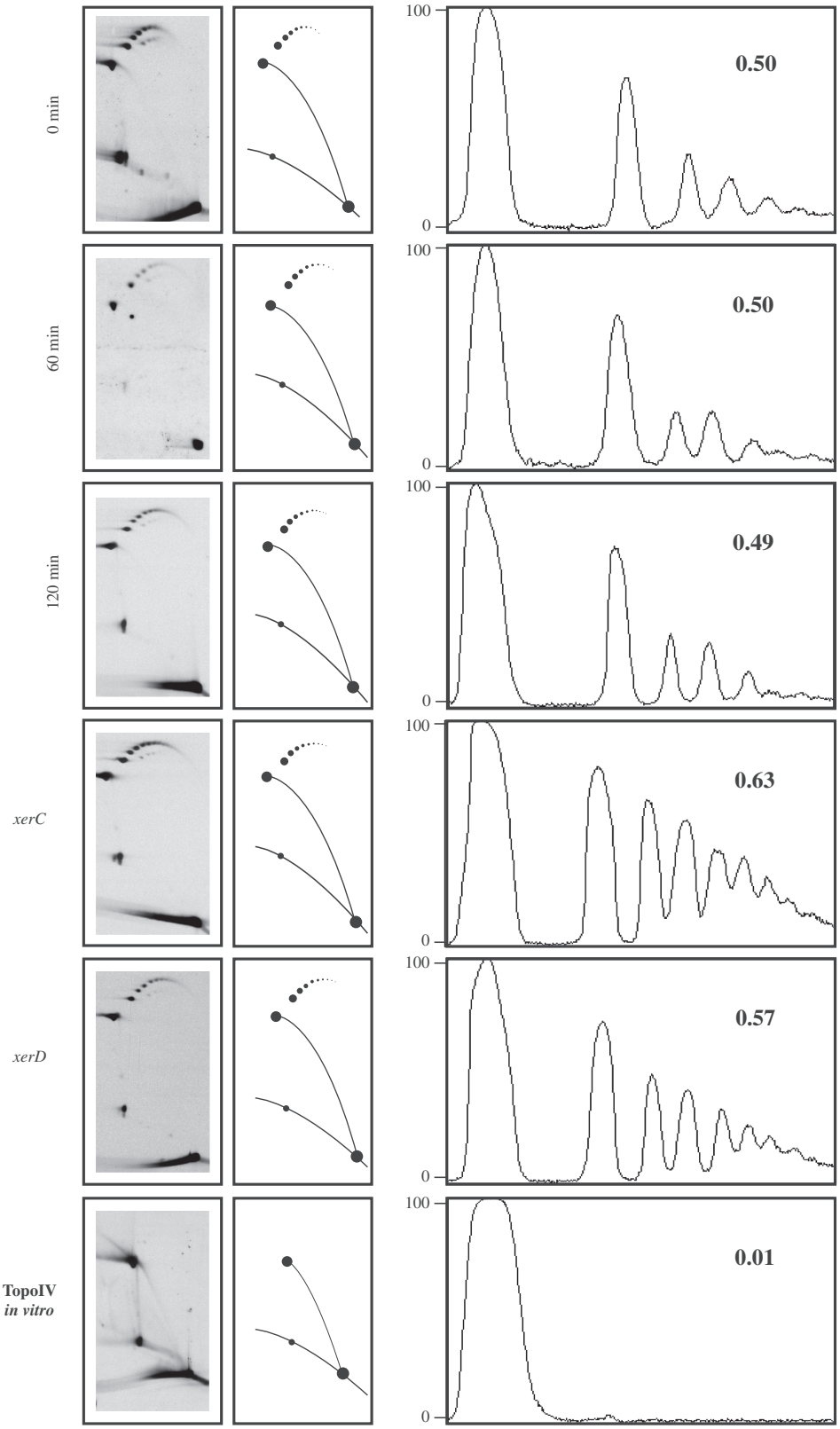

Figure 7. The frequency of knotted RIs remains unchanged after inhibition of Topo IV as well as in *xerC*/*xerD* mutants. Autoradiograms of 2D gels corresponding to pBR-TerE@DraI isolated from parE10 *E. coli* cells grown at the permissive temperature (30°C), and 60 and 120 min after shifting the culture to the restrictive temperature (43°C). DNA was digested with AlwNI and the portion of each autoradiogram where unknotted and knotted RIs migrated was scanned and analysed by densitometry. The corresponding densitometric profiles are shown to the right. The numbers at the top right corner of each profile indicate the ratio of knotted/unknotted molecules in each case. Note that this ratio did not change significantly with time at the restrictive temperature or when plasmid DNA was isolated from *xerC* or *xerD* mutant cells. On the contrary, exposure of plasmid DNA to Topo IV *in vitro* resulted in the elimination of almost all knotted to unknotted forms (shown at the bottom).

in Figure 7 indicated that this ratio remained unchanged. Therefore one must conclude that XerC and XerD are not involved in the formation of these interchromatid knots. To confirm that Topo IV was indeed capable to remove the knots, a DNA sample identical to the one labelled 120 min in this figure was exposed to Topo IV *in vitro* after its digestion with AlwNI. The result obtained is shown at the bottom of Figure 7. Almost all knotted forms disappeared and the only molecular species remaining corresponded to unknotted RIs. There is only one way to explain all the results obtained so far. Topo IV is responsible for knotting as well as for unknotting RIs. When Topo IV is inhibited, both the formation as well as the removal of these knots decline and the ratio of knotted to unknotted RIs remains unchanged.

DISCUSSION

Why and how does Topo IV cause the formation of replication knots? Mechanistically, one possibility is diagrammed in Figure 8. For a half replicated molecule (A), the unreplicated portion is negatively supercoiled and the parental duplex winds around itself in a right-handed manner. In the replicated portion on the other hand, the sister duplexes wind in a left-handed manner (1). It was recently suggested that Topo IV is processive on right-handed crosses and distributive on left-handed ones (35). This would definitively affect Topo IV function on highly intertwined precatenanes but not necessarily when sister duplexes are poorly intertwined (28). Indeed, the formation of interchromatid knots during replication (13) and the geometry of RIs cut by poisoning topo II with etoposide (36) are the best experimental evidences supporting the existence of precatenanes *in vivo* (37). A single passage of one of the duplexes that traps two precatenane nodes (Figure 8B and C) would generate a trefoil interchromatid knot (Figure 8D) which becomes simplified by linearization of the molecule with a single double-stranded cut in the unreplicated portion. Of course, this is the simplest way to generate an interchromatid knot. More DNA passages would lead to the whole spectrum of knots observed *in vivo*. Moreover, it is well known that varying levels of positive and negative supercoiling differently affect the efficiency with which Topo IV catenanes and decatenanes DNA (38) and the unique mode of clamping the right-handed nodes by Topo IV establishes a different topological link with positive and negative supercoiled DNA (39). It was recently shown that during unconstrained replication sister duplexes are highly intertwined (28). Here we propose that when replication forks slow down or stall, sister duplexes become loosely intertwined. Under these conditions Topo IV could inadvertently make the strand passages that lead to the formation of inter- and intrachromatid knots that must be removed later on to allow their correct segregation. In other words, we suggest that during unconstrained replication the strong intertwining of sister duplexes prevents the formation of these potentially harmful knots. This role of strong intertwining of sister duplexes would be similar to the role of negative supercoiling for preventing potentially harmful DNA–DNA intersegmental contacts and wrong strand-passage reactions as previously suggested (40–42).

Intrachromatid knots have been described and analysed in pBR322 catenanes before (16). Although it was found that Topo IV inactivation had a surprisingly minor role on the level of these intrachromatid knotted catenanes, the authors avoided to make any comment as to their origin. Here we demonstrated that inter- as well as intrachromatid knots form during DNA replication. Once replication is over, though, the fate of these two types of knots differs. Interchromatid knots automatically

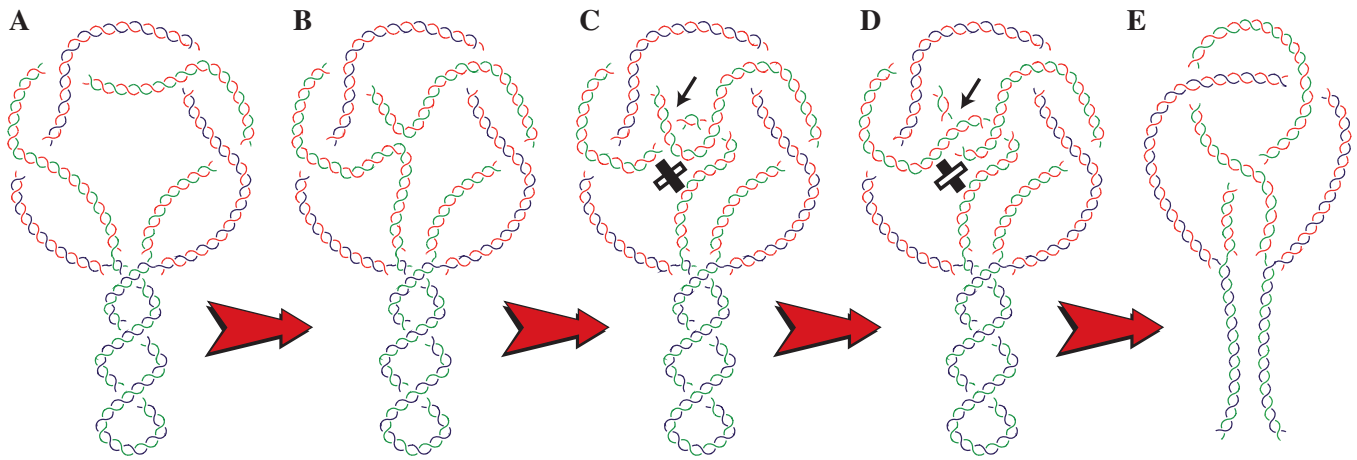

Figure 8. A single inadvertent passage performed by Topo IV can convert precatenanes into an interchromatid trefoil knot. (**A**) Half-replicated molecule showing that in the unreplicated portion the parental duplex wounds in a right-handed manner whereas sister duplexes wound in a left-handed manner in the replicated portion. (**B**) Two segments of the same chromatid that are separated by two precatenane nodes approximate to each other and become crossed (**C**). The inadvertent passage performed by Topo IV (C to D transition) converts this precatenated RI into a molecule with an interchromatid knot (**D**). The resulting trefoil knot is fully revealed if the molecule is digested with a restriction enzyme that linearize the RI at the unreplicated portion, leading to the elimination of supercoiling in the unreplicated portion and all remaining precatenane nodes (**E**). Parental duplexes are drawn in blue and green whereas nascent strands are depicted in red. The arrows and black and white segments in C and D point to the single inadvertent passage performed by Topo IV.

give rise to catenanes undistinguishable from those derived from precatenanes. Intrachromatid knots, on the other hand, could persist and generate the knotted catenanes described by Adams *et al.* (16). It is interesting to note that our proposal that knotting increases in RIs with loosely intertwined sister duplexes, could also explain the observation that DNA gyrase inhibitors increase the content of knots in non-replicating bacterial plasmids (7–9). The inhibition of gyrase causes DNA relaxation and in poorly supercoiled plasmids, Topo IV could also inadvertently make the strand passages that lead to the formation of knots. Indeed, numerical simulations already suggested that DNA supercoiling has a significant role in DNA unknotting (4,41,42).

Finally, all these observations together with the finding that cohesion also plays a significant role in decatenation in eukaryotes (43) give rise to several new questions: Does interchromatid knots form also in eukaryotic linear chromosomes? Does topoisomerase II, the eukaryotic decatenase, leads also to the formation of this type of knots when replication forks slowdown or stall in eukaryotes? New experiments are underway to solve these and other related topics.

SUPPLEMENTARY DATA

Supplementary Data are available at NAR Online: Supplementary Table 1.

ACKNOWLEDGEMENTS

The authors acknowledge Estefanía Monturus de Carandini, María Rodríguez, Marta Fierro-Fernández, Doris Gómez, María Tenorio and Zaira García for their suggestions and support during the course of this study. They also thank Lynn Zechiedrich, Ian Grainge and Kenneth Marians for bacterial strains. They are truly indebted to Guillaume Witz and Giovanni Dietler for introducing them to AFM and Victor Muñoz for sharing the AFM facilities at the CIB. Finally, they could not accomplish this work without the continuous support and constructive criticism of Andrzej Stasiak. V.L. performed all the experiments with the help of M.L.M.R. P.H. and D.B.K. analysed the results and discussed the manuscript. J.B.S. designed the experiments, analysed the results and wrote the manuscript.

FUNDING

Funding for open access charge: Spanish Ministerio de Ciencia e Innovación (grants BFU2008-00408/BMC and BFU2011-22489BMC to J.B.S.).

Conflict of interest statement. None declared.

REFERENCES

1. Schvartzman,J.B. and Stasiak,A. (2004) A topological view of the replicon. *EMBO Rep.*, **5**, 256–261.
2. Wang,J. (2009) *Untangling the Double Helix*. Cold Spring Harbor Laboratory Press, New York.
3. Delbrück,M. (1962) Knotting problems in Biology. *Proc. Symp. Appl. Math.*, **14**, 55–63.
4. Witz,G. and Stasiak,A. (2010) DNA supercoiling and its role in DNA decatenation and unknotting. *Nucleic Acids Res.*, **38**, 2119–2133.
5. Ashley,C. and Lee,J.S. (2000) A triplex-mediated knot between separated polypurine-polypyrimidine tracts in circular DNA blocks transcription by *Escherichia coli* RNA polymerase. *DNA Cell Biol.*, **19**, 235–241.
6. Portugal,J. and RodriguezCampos,A. (1996) T7 RNA polymerase cannot transcribe through a highly knotted DNA template. *Nucleic Acids Res.*, **24**, 4890–4894.
7. Shishido,K., Ishii,S. and Komiyaba,N. (1989) The presence of the region on pBR322 that encodes resistance to tetracycline is responsible for high levels of plasmid DNA knotting in *Escherichia coli* DNA topoisomerase I deletion mutant. *Nucleic Acids Res.*, **17**, 9749–9759.
8. Shishido,K., Komiyama,M. and Ikawa,S. (1987) Increased production of a knotted form of plasmid pBR322 DNA in *Escherichia coli* DNA topoisomerase mutants. *J. Mol. Biol.*, **195**, 215–218.
9. Ishii,S., Murakami,T. and Shishido,K. (1991) Gyrase inhibitors increase the content of knotted DNA species of plasmid pBR322 in *Escherichia coli*. *J. Bac*, **173**, 5551–5553.
10. Olavarrieta,L., Hernández,P., Krimer,D.B. and Schvartzman,J.B. (2002) DNA knotting caused by head-on collision of transcription and replication. *J. Mol. Biol.*, **322**, 1–6.
11. Olavarrieta,L., Martínez-Robles,M.L., Hernández,P., Krimer,D.B. and Schvartzman,J.B. (2002) Knotting dynamics during DNA replication. *Mol. Microbiol.*, **46**, 699–707.
12. Olavarrieta,L., Martinez-Robles,M.L., Sogo,J.M., Stasiak,A., Hernandez,P., Krimer,D.B. and Schvartzman,J.B. (2002) Supercoiling, knotting and replication fork reversal in partially replicated plasmids. *Nucleic Acids Res.*, **30**, 656–666.
13. Sogo,J.M., Stasiak,A., Martínez-Robles,M.L., Krimer,D.B., Hernández,P. and Schvartzman,J.B. (1999) Formation of knots in partially replicated DNA molecules. *J. Mol. Biol.*, **286**, 637–643.
14. Viguera,E., Hernández,P., Krimer,D.B., Boistov,A.S., Lurz,R., Alonso,J.C. and Schvartzman,J.B. (1996) The ColE1 unidirectional origin acts as a polar replication fork pausing site. *J. Biol. Chem.*, **271**, 22414–22421.
15. Dean,F.B., Stasiak,A., Koller,T. and Cozzarelli,N.R. (1985) Duplex DNA knots produced by *Escherichia coli* topoisomerase I. *J. Biol. Chem.*, **260**, 4975–4983.
16. Adams,D.E., Shekhtman,E.M., Zechiedrich,E.L., Schmid,M.B. and Cozzarelli,N.R. (1992) The role of topoisomerase-IV in partitioning bacterial replicons and the structure of catenated intermediates in DNA replication. *Cell*, **71**, 277–288.
17. Buck,G.R. and Zechiedrich,E.L. (2004) DNA disentangling by type-2 topoisomerases. *J. Mol. Biol.*, **340**, 933–939.
18. Deibler,R.W., Rahmati,S. and Zechiedrich,E.L. (2001) Topoisomerase IV, alone, unknots DNA in *E. coli*. *Genes Dev*, **15**, 748–761.
19. Zechiedrich,E.L. and Cozzarelli,N.R. (1995) Roles of topoisomerase IV and DNA gyrase in DNA unlinking during replication in *Escherichia coli*. *Genes Dev.*, **9**, 2859–2869.
20. Zechiedrich,E.L., Khodursky,A.B. and Cozzarelli,N.R. (1997) Topoisomerase IV, not gyrase, decatenates products of site-specific recombination in *Escherichia coli*. *Genes Dev.*, **11**, 2580–2592.
21. Bastia,D. and Mohanty,B.K. (1996) Mechanisms for completing DNA replication. In: DePamphilis,M.L. (ed.), *DNA Replication in Eukaryotic Cells*. Cold Spring Harbor Laboratory Press, New York, pp. 177–215.
22. Hill,T.M., Pelletier,A.J., Tecklenburg,M.L. and Kuempel,P.L. (1988) Identification of the DNA sequence from E. coli terminus region that halts replication forks. *Cell*, **55**, 459–466.
23. Santamaría,D., Hernández,P., Martínez-Robles,M.L., Krimer,D.B. and Schvartzman,J.B. (2000) Premature termination of DNA replication in plasmids carrying two inversely oriented ColE1 origins. *J. Mol. Biol.*, **300**, 75–82.
24. Sattin,B.D. and Goh,M.C. (2004) Direct observation of the assembly of RecA/DNA complexes by atomic force microscopy. *Biophys. J.*, **87**, 3430–3436.

25. Santamaría,D., delaCueva,G., Martínez-Robles,M.L., Krimer,D.B., Hernández,P. and Schvartzman,J.B. (1998) DnaB helicase is unable to dissociate RNA-DNA hybrids—its implication in the polar pausing of replication forks at ColE1 origins. *J. Biol. Chem.*, **273**, 33386–33396.
26. Hirota,Y., Ryter,A. and Jacob,F. (1968) Thermosensitive mutants of E. coli affected in the processes of DNA synthesis and cellular division. *Cold Spring Harb. Symp. Quant. Biol.*, **33**, 677–693.
27. Kato,J., Nishimura,Y., Imamura,R., Niki,H., Hiraga,S. and Suzuki,H. (1990) New topoisomerase essential for chromosome segregation in *E. coli*. *Cell*, **63**, 393–404.
28. Martinez-Robles,M.L., Witz,G., Hernandez,P., Schvartzman,J.B., Stasiak,A. and Krimer,D.B. (2009) Interplay of DNA supercoiling and catenation during the segregation of sister duplexes. *Nucleic Acids Res.*, **37**, 5126–5137.
29. Fierro-Fernandez,M., Hernandez,P., Krimer,D.B. and Schvartzman,J.B. (2007) Replication fork reversal occurs spontaneously after digestion but is constrained in supercoiled domains. *J. Biol. Chem.*, **282**, 18190–18196.
30. Fierro-Fernandez,M., Hernandez,P., Krimer,D.B., Stasiak,A. and Schvartzman,J.B. (2007) Topological locking restrains replication fork reversal. *Proc. Natl Acad. Sci. USA*, **104**, 1500–1505.
31. Viguera,E., Hernandez,P., Krimer,D.B., Lurz,R. and Schvartzman,J.B. (2000) Visualisation of plasmid replication intermediates containing reversed forks. *Nucleic Acids Res.*, **28**, 498–503.
32. Peter,B.J., Ullsperger,C., Hiasa,H., Marians,K.J. and Cozzarelli,N.R. (1998) The structure of supercoiled intermediates in DNA replication. *Cell*, **94**, 819–827.
33. Martin-Parras,L., Lucas,I., Martinez-Robles,M.L., Hernandez,P., Krimer,D.B., Hyrien,O. and Schvartzman,J.B. (1998) Topological complexity of different populations of pBR322 as visualized by two-dimensional agarose gel electrophoresis. *Nucleic Acids Res.*, **26**, 3424–3432.
34. Grainge,I., Bregu,M., Vazquez,M., Sivanathan,V., Ip,S.C. and Sherratt,D.J. (2007) Unlinking chromosome catenanes in vivo by site-specific recombination. *EMBO J.*, **26**, 4228–4238.
35. Neuman,K.C., Charvin,G., Bensimon,D. and Croquette,V. (2009) Mechanisms of chiral discrimination by topoisomerase IV. *Proc. Natl Acad. Sci. USA*, **106**, 6986–6991.
36. Lucas,I., Germe,T., Chevrier-Miller,M. and Hyrien,O. (2001) Topoisomerase II can unlink replicating DNA by precatenane removal. *EMBO J.*, **20**, 6509–6519.
37. Postow,L., Peter,B.J. and Cozzarelli,N.B. (1999) Knot what we thought before: the twisted story of replication. *Bioessays*, **21**, 805–808.
38. Roca,J. (2001) Varying levels of positive and negative supercoiling differently affect the efficiency with which topoisomerase II catenates and decatenates DNA. *J. Mol. Biol.*, **305**, 441–450.
39. Timsit,Y. (2011) Local sensing of global DNA topology: from crossover geometry to type II topoisomerase processivity. *Nucleic Acids Res.*, **39**, 8665–8676.
40. Timsit,Y. and Varnai,P. (2010) Helical chirality: a link between local interactions and global topology in DNA. *PLoS One*, **5**, e9326.
41. Witz,G., Dietler,G. and Stasiak,A. (2011) DNA knots and DNA supercoiling. *Cell Cycle*, **10**, 1339–1340.
42. Witz,G., Dietler,G. and Stasiak,A. (2011) Tightening of DNA knots by supercoiling facilitates their unknotting by type II DNA topoisomerases. *Proc. Natl Acad. Sci. USA*, **108**, 3608–3611.
43. Farcas,A.M.P.U., Helmhart,W. and Nasmyth,K. (2011) Cohesin's concatenation of sister DNAs maintains their intertwining. *Mol. Cell*, **44**, 97–107.